A numerical investigation of stability of 1D soliton solutions of Boussinesq paradigm equation in the 2D case

Daniela Vasileva

Institute of Mathematics and Informatics,
Bulgarian Academy of Sciences

1. Motivation
2. Numerical method for solving BPE in a moving frame coordinate system
3. Properties of the finite difference scheme
4. Numerical Experiments
5. Conclusion

Motivation

- The several variants of Boussinesq equation (BE) model surface waves in shallow fluid layer. One important feature of BE is the balance between the nonlinearity and dispersion, which leads to solutions of type of permanent waves (solitons).

  J. V. Boussinesq, Théorie des ondes et des remous qui se propagent le long d'un canal rectangulaire horizontal, en communiquant au liquide contenu dans ce canal des vitesses sensiblement pareilles de la surface au fond, Journal de Mathématiques Pures et Appliquées 17 (1872) 55–108.

- The accurate derivation of the Boussinesq system combined with an approximation, that reduces the full model to a single equation, leads to the Boussinesq Paradigm Equation (BPE)

$$u_{tt} = \Delta \left[u - F(u) + \beta_1 u_{tt} - \beta_2 \Delta u \right], \quad F(u) := \alpha u^2,$$

  where u is the surface elevation, $\beta_1 > 0$, $\beta_2 > 0$ – dispersion coefficients, $\alpha > 0$ – amplitude parameter, $\beta_2 = \alpha = 1$ without loosing of generality.

  C. I. Christov, An energy-consistent Galilean-invariant dispersive shallow-water model, Wave Motion 34 (2001) 161–174.

- 2D BPE admits stationary translating soliton solutions, which can be constructed using either finite differences, perturbation technique, or Galerkin spectral method:

  J. Choudhury, C.I. Christov, 2D solitary waves of Boussinesq equation. APS Conference Proceedings 755 (2005), 85–90.

  C. I. Christov, Numerical implementation of the asymptotic boundary conditions for steadily propagating 2D solitons of Boussinesq type equations, Math. Comp. Simulat. 82 (2012) , 1079–1092.

  C. I. Christov, J. Choudhury, Perturbation solution for the 2D shallow-water waves, Mech. Res. Commun. 38 (2011) 274–281.

  C.I. Christov, M.T. Todorov, M.A. Christou, Perturbation solution for the 2D shallow-water waves. AIP Conference Proceedings 1404 (2011), 49–56.

  M.A. Christou, C.I. Christov, Fourier-Galerkin method for 2D solitons of Boussinesq equation, Math. Comput. Simul. 74 (2007) 82–92.

- Results about the time evolution and structural stability of the initial data, obtained using the perturbation technique, are presented in

  A. Chertock, C. I. Christov, A. Kurganov, Central-upwind schemes for the Boussinesq paradigm equation. Computational Science and High Performance Computing IV, NNFM, 113, 267–281 (2011).

C.I. Christov, N. Kolkovska, D. Vasileva, On the numerical simulation of unsteady solutions for the 2D Boussinesq paradigm equation, Lecture Notes Computer Science 6046 (2011), 386–394.

C.I. Christov, N. Kolkovska, D. Vasileva, Numerical investigation of unsteady solutions for the 2D Boussinesq paradigm equation, 5th Annual Meeting of the Bulgarian Section of SIAM, BGSIAM'10 Proceedings (2011), 11–16.

M. Dimova, D. Vasileva, Comparison of two numerical approaches to Boussinesq paradigm equation, Lecture Notes Computer Science 8236 (2013), 255–262.

using different numerical methods. All results are in good agreement and show that the 2D localized soliton solutions are not stable – they either disperse in the form of ring-waves or blow-up (depending on the parameters).

- We continued the investigations using a moving frame coordinate system. It allows us to keep the localized structure in the center of the coordinate system, to use a small computational box and to compute the solution for larger times. The same unstable bahaviour of the 2D localized soliton solutions was demonstrated in

  D. Vasileva, C.I. Christov, On the numerical investigation of unsteady solutions for the 2D Boussinesq paradigm equation in a moving frame coordinate system, 6th Annual Meeting of the Bulgarian Section of SIAM, BGSIAM'11 Proceedings (2012), 103–108.

- This motivated us to investigate the question about the time behaviour of known stable 1D solitons, but when they are taken as initial data in 2D problems.

- The BPE is transformed in order to keep the soliton in the center of the new coordinate system – we set $z := x - ct$, where c is the velocity of the stationary propagating soliton. Then the following equation for $U(z, y, t) := u(z + ct, y, t)$ is obtained in the moving frame coordinate system

$$(I - \beta_1 \tilde{\Delta}) \frac{\partial^2 U}{\partial t^2} - 2c \frac{\partial^2 U}{\partial t \partial z} + 2c\beta_1 \frac{\partial^2}{\partial t \partial z} \tilde{\Delta} U = -\beta_2 \frac{\partial^4 U}{\partial y^4} - (2\beta_2 - \beta_1 c^2) \frac{\partial^4 U}{\partial y^2 \partial z^2}$$
$$- (\beta_2 - \beta_1 c^2) \frac{\partial^4 U}{\partial z^4} + \frac{\partial^2 U}{\partial y^2} + (1 - c^2) \frac{\partial^2 U}{\partial z^2} - \alpha \tilde{\Delta} F(U).$$

Here I is the identity operator and $\tilde{\Delta}$ stands for the Laplace operator with respect to variables z and y. The fourth order spatial derivatives in the right hand side constitute a fourth order elliptic operator if $c^2 < \beta_2/\beta_1$. In a similar way the second order derivatives generate a second order elliptic operator if $c^2 < 1$. Therefore we suppose in the following that the velocity c satisfies the restriction $c^2 < \min(1, \beta_2/\beta_1)$.

Numerical method for solving BPE in the moving frame coordinate system

We introduce the following new dependent function $W(z,y,t) := U - \beta_1 \tilde{\Delta} U$ and get the following equation for W

$$W_{tt} - 2cW_{tz} + c^2 W_{zz} = \frac{\beta_2}{\beta_1}\tilde{\Delta} W + \frac{\beta_1 - \beta_2}{\beta_1^2}(U - W) - \tilde{\Delta} F(U).$$

Thus we obtain a system consisting of an equation for U and an equation for W.

The following implicit time stepping is designed for this system

$$\frac{W_{ij}^{n+1} - 2W_{ij}^n + W_{ij}^{n-1}}{\tau^2} - c\frac{V^z[W_{ij}^{n+1} - W_{ij}^{n-1}]}{\tau} + \frac{c^2}{2}\Lambda^{zz}[W_{ij}^{n+1} + W_{ij}^{n-1}]$$
$$= \frac{\beta_2}{2\beta_1}\Lambda\left[W_{ij}^{n+1} + W_{ij}^{n-1}\right] + \frac{\beta_1 - \beta_2}{2\beta_1^2}[U_{ij}^{n+1} - W_{ij}^{n+1} + U_{ij}^{n-1} - W_{ij}^{n-1}]$$
$$- \alpha\Lambda G(U_{ij}^{n+1}, U_{ij}^n, U_{ij}^{n-1}),$$
$$U_{ij}^{n+1} - \beta_1 \Lambda U_{ij}^{n+1} = W_{ij}^{n+1}, \quad i = 1, \ldots, N_z - 1, \quad j = 1, \ldots, N_y - 1.$$

Here τ is the time increment, the nonlinear term U^2 is approximated by

$$G(U_{ij}^{n+1}, U_{ij}^{n}, U_{ij}^{n-1}) = (U_{ij}^{n})^2 \quad \text{or}$$

$$G(U_{ij}^{n+1}, U_{ij}^{n}, U_{ij}^{n-1}) = \left[(U_{ij}^{n+1})^2 + U_{ij}^{n+1}U_{ij}^{n-1} + (U_{ij}^{n-1})^2\right]/3,$$

$\Lambda = \Lambda^{zz} + \Lambda^{yy}$ stands for the difference approximation of the Laplace operator $\tilde{\Delta}$ on a non-uniform grid, for example

$$\Lambda^{zz} W_{ij} = \frac{2W_{i-1j}}{h_{i-1}^z(h_i^z + h_{i-1}^z)} - \frac{2W_{ij}}{h_i^z h_{i-1}^z} + \frac{2W_{i+1j}}{h_i^z(h_i^z + h_{i-1}^z)},$$

and V^z is a central difference approximation of $\frac{\partial}{\partial z}$

$$V_z W_{ij} = \frac{h_{i-1}^z W_{i+1j}}{h_i^z(h_i^z + h_{i-1}^z)} - \frac{h_i^z W_{i-1j}}{h_{i-1}^z(h_i^z + h_{i-1}^z)} + \frac{(h_i^z - h_{i-1}^z)W_{ij}}{h_i^z h_{i-1}^z}.$$

Another way to approximate W_{zt} for $c > 0$ is by the following "upwind"

approximation

$$W_{zt} \approx \frac{W_{i+1j}^{n+1} - W_{ij}^{n+1} - W_{i+1j}^{n} + W_{ij}^{n}}{2\tau h_i^z} + \frac{W_{ij}^{n} - W_{i-1j}^{n} - W_{ij}^{n-1} + W_{i-1j}^{n-1}}{2\tau h_{i-1}^z}.$$

The values of the sought functions at the $(n-1)$-st and n-th time stages are considered as known when computing the $(n+1)$-st stage. When the approximation G of the nonlinear term U^2 includes the $n+1$-st level, the system is linearized using internal (Picard) iterations, i.e., we perform successive iterations for W and U on the $(n+1)$-st stage, starting with initial approximation from the already computed n-th stage. Usually 5-10 nonlinear iterations are sufficient for convergence with tolerance 10^{-14}.

The following quasi-uniform grid is used in the $z-$direction

$$z_i = \sinh[\hat{h}_z(i - n_z)],\ z_{N_z-i} = -z_i,\ i = n_z + 1, \ldots, N_z,\ z_{n_z} = 0,$$

where N_z is an even number, $n_z = (N_z)/2$, $\hat{h}_z = D_z/(N_z - 1)$, and D_z is selected in a manner to have large enough computational region. The grid in the $y-$direction is uniform.

In order to test the properties of the numerical method, we take the known one-dimensional solutions of the problem as initial data:

$$U(z,y,0) = U^{\mathrm{sech}}(z) = (1-c^2)\frac{1.5}{\alpha}\mathrm{sech}^2\big(0.5z\sqrt{(1-c^2)/(\beta_2-\beta_1 c^2)}\big).$$

The second initial condition is chosen as $\dfrac{\partial}{\partial t}U(z,y,0) = 0.$

Because of the localization of the wave profile in the $z-$direction, the boundary conditions in this direction can be set equal to zero, when the size of the computational domain is large enough. Neumann boundary conditions are imposed in the $y-$direction.

The coupled system of equations is solved by the Bi-Conjugate Gradient Stabilized Method with ILU preconditioner. In most examples we set the tolerance for the iterative solution of the linear systems to be 10^{-14}.

Properties of the finite difference schemes

Theoretical analysis of the linear schemes (function G independent on U) corresponding to both FDS as well as numerical tests about the convergence and stability of the nonlinear schemes:

D. Vasileva, N. Kolkovska, Investigation of Two Numerical Schemes for the 2D Boussinesq Paradigm Equation in a Moving Frame Coordinate System, 8th Annual Meeting of the Bulgarian Section of SIAM, to appear in BGSIAM'13 Proceedings

Theorem 1. *Let* $c^2 < \min(1, \beta_2/\beta_1)$. *Then the finite difference schemes are stable with respect to the initial data and the function* G. *Moreover, the following estimate holds*

$$\left((-\Lambda)U^{(n)}, U^{(n)}\right) \leq C \left[\left((-\Lambda)U^{(0)}, U^{(0)}\right) + \left((-\Lambda)^{-1} B U_t^{(0)}, U_t^{(0)}\right) + \sum_{m=1}^{n} \tau \left(G^m, G^m\right)\right]$$

with a constant C *independent on* U, h *and* τ.

Numerical experiments

In Bona, J., Sachs, R.: Global existence of smooth solutions and stability of solitary waves for a generalized Boussinesq equation, Comm. Math. Phys., 118, 15–29 (1988) it is proved that the aforementioned soliton solutions of the 1D generalized Boussinesq equation ($\beta_2 = \alpha = 1,\ \beta_1 = 0$) are stable when $0.25 < c^2 < 1$.

In Liu, Y: Instability of solitary waves for generalized Boussinesq equations, J. Dynamics Differential Equations, 5, 537–558 (1993) nonlinear instability is obtained when $c^2 \leq 0.25$. In our numerical experiments we observe a similar behaviour for the 1D BPE, i.e., when $\beta_1 = 1$. That is why in the next examples solutions for $\beta_1 = \beta_2 = \alpha = 1$ are investigated.

Example 1. $c = 0.4$ (1D soliton solution should be unstable).

The basic 2D grid has 256×16 cells in $[-50, 50] \times [-1, 1]$, the time step is $\tau = 0.2$.

We compare the solution in the 2D setting with the 1D solution, computed on a grid with 256 cells in the interval $[-50, 50]$ and with the same time step $\tau = 0.2$.

The numerical solutions are computed using the approximation on the $n-$th level of the nonlinear term.

Table 1: The difference $\delta(U) := \max |U - U^{\mathrm{sech}}|$ between the exact and the numerical solution for $c = 0.4$

	central differences		upwind differences	
t	2D solution	1D solution	2D solution	1D solution
8	1.57e-3	1.57e-3	1.57e-3	1.57e-3
16	5.59e-3	5.59e-3	5.60e-3	5.60e-3
24	1.43e-2	1.43e-2	1.44e-2	1.44e-2
32	3.15e-2	3.15e-2	3.16e-2	3.16e-2
40	6.45e-2	6.45e-2	6.49e-2	6.49e-2
48	1.29e-1	1.29e-1	1.30e-1	1.30e-1
56	2.63e-1	2.63e-1	2.66e-1	2.66e-1
64	5.93e-1	5.93e-1	6.01e-1	6.01e-1
72	2.41	2.41	2.51	2.51
75	56.61	56.61	83.54	83.54
76	1.22e+11	1.22e+11	1.48e+14	1.48e+14

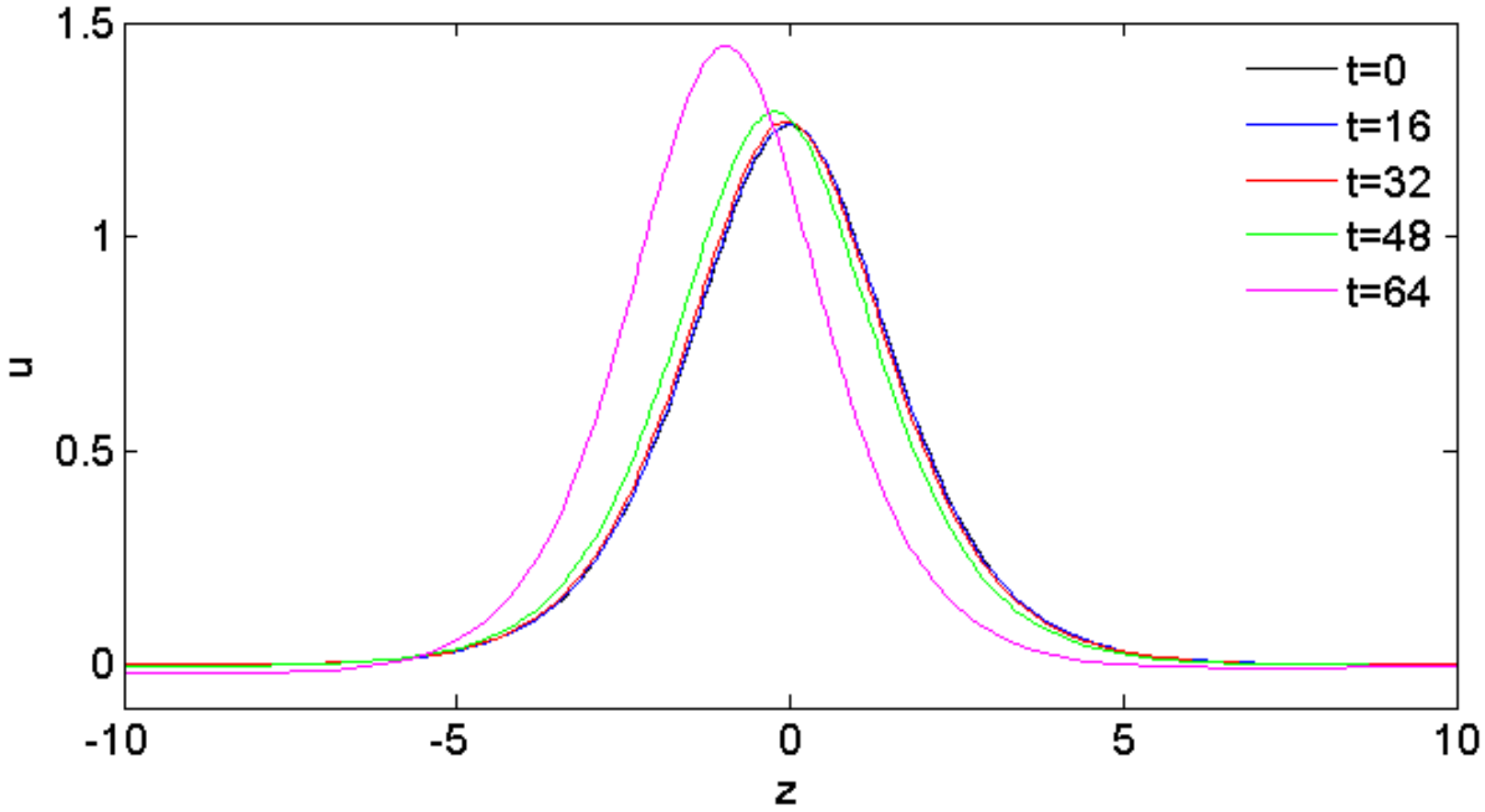

Figure 1: Evolution of the 1D solution for $c = 0.4$.

The evolution of the cross-sections of the 2D solution is the same, because the 2D solution keeps its constant behaviour in the $y-$direction.

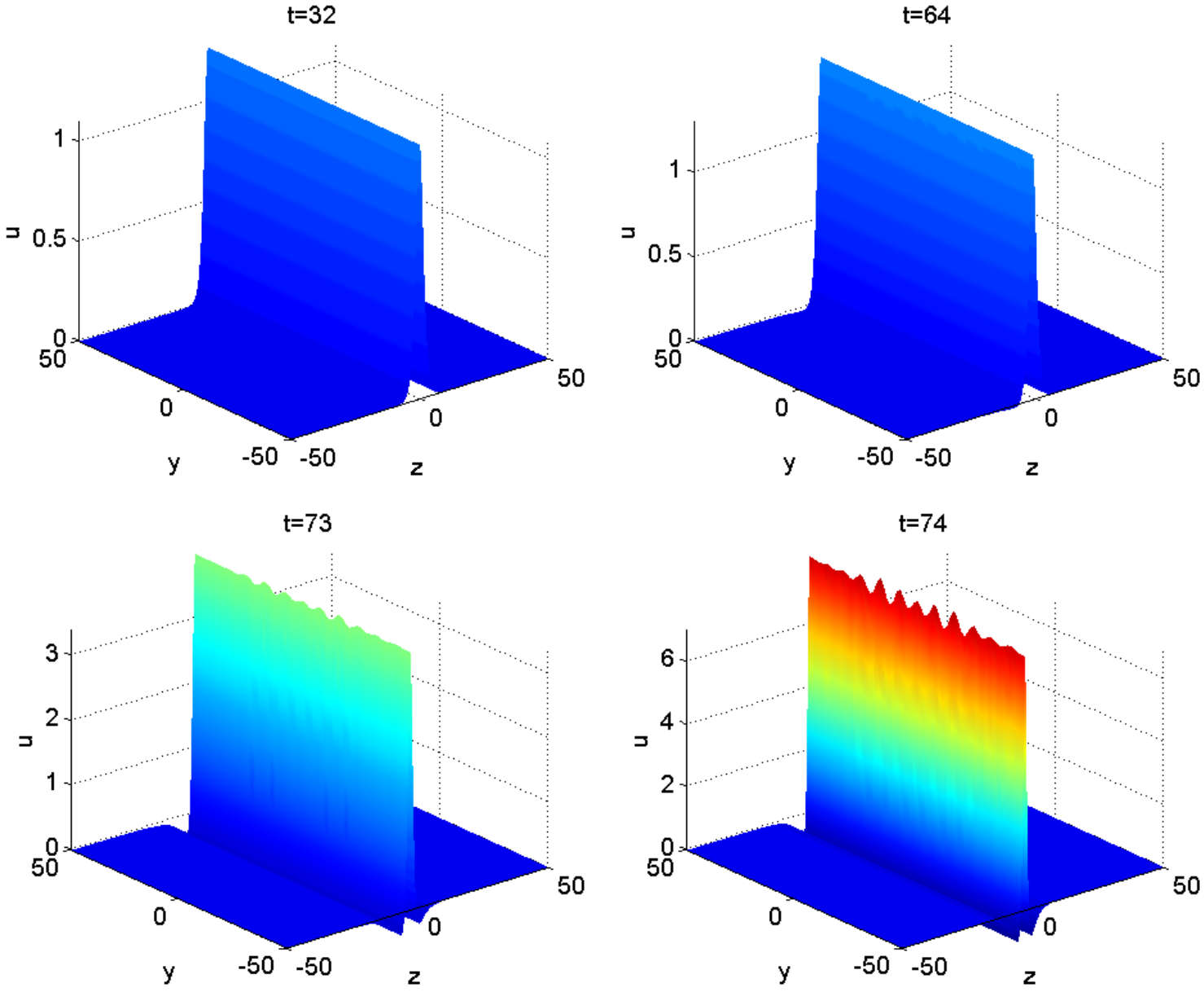

Figure 2: Evolution of the 2D solution for $c = 0.4$, $y \in [-50, 50]$.

Example 2. $c = 0.6$ (1D soliton solution should be stable).

The basic 2D grid has 256×16 cells in $[-50, 50] \times [-1, 1]$, the time step is $\tau = 0.2$.

Table 2: The difference $\delta(U) := \max |U - U^{\mathrm{sech}}|$ between the exact and the numerical solution for $c = 0.6$

	central differences		upwind differences	
t	2D solution	1D solution	2D solution	1D solution
10^2	5.15e-3	5.15e-3	5.16e-2	5.16e-3
10^3	9.73e-3	9.73e-3	9.66e-3	9.66e-3
10^4	1.80e-2	1.80e-2	1.83e-2	1.83e-2
10^5	1.05e-2	1.05e-2	6.94e-3	6.94e-3
10^6	1.01e-2	1.01e-2	8.49e-3	8.49e-3

Both approximations of the nonlinear term, as well as a stronger tolerance for the iterative solution of the linear systems (10^{-28}) also lead to practically the same results.

We also investigate the convergence of the 2D solution on three grids – the basic grid has 256×8 cells, $\tau = 0.2$, the finer has 512×16 cells, $\tau = 0.1$, the finest has 1024×32 cells, $\tau = 0.05$.

The order of convergence l is computed as $l = \log_2 \frac{\delta(U_{k-1})}{\delta(U_k)}$, where k is the number of the corresponding grid.

The central difference and upwind approximations of W_{tz} lead to practically the same values in the numerical solution.

Both approximations of the nonlinear term as well as a stronger tolerance for the iterative solution of the linear systems (10^{-28}) also lead to practically the same results.

Table 3: The difference $\delta(U)$ between the exact and the numerical solution, and the order of convergence l for $c = 0.6$

		$t = 100$		$t = 200$		$t = 400$	
τ	$N_x \times N_y$	$\delta(U)$	l	$\delta(U)$	l	$\delta(U)$	l
central differences, first approximation of the nonlinear term							
0.2	256×8	5.15e-3		9.50e-3		1.67e-2	
0.1	512×16	1.30e-3	1.99	2.46e-3	1.95	4.83e-3	1.79
0.05	1024×32	3.26e-4	2.00	6.20e-4	1.99	1.25e-3	1.95
central differences, second approximation of the nonlinear term							
0.2	256×8	5.15e-3		9.50e-3		1.67e-2	
0.1	512×16	1.30e-3	1.99	2.46e-3	1.95	4.83e-3	1.79
0.05	1024×32	3.26e-4	2.00	6.20e-4	1.99	1.25e-3	1.95
upwind differences, first approximation of the nonlinear term							
0.2	256×8	5.16e-3		9.52e-3		1.67e-2	
0.1	512×16	1.30e-3	1.99	2.46e-3	1.95	4.83e-3	1.79
0.05	1024×32	3.26e-4	2.00	6.20e-4	1.99	1.25e-3	1.95
upwind differences, second approximation of the nonlinear term							
0.2	256×8	5.15e-3		9.52e-3		1.67e-2	
0.1	512×16	1.30e-3	1.99	2.46e-3	1.95	4.83e-3	1.79
0.05	1024×32	3.26e-4	2.00	6.20e-4	1.99	1.25e-3	1.95

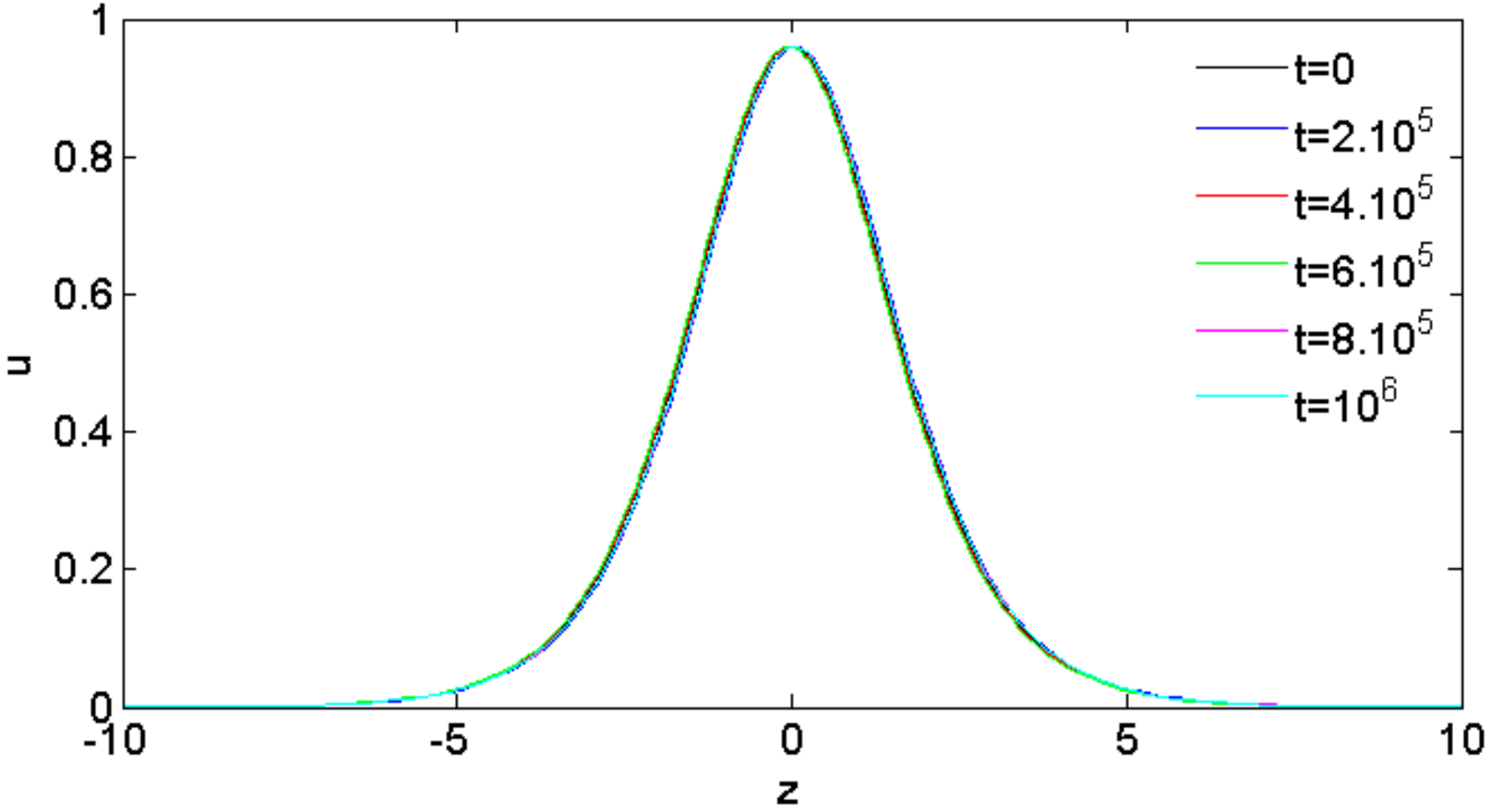

Figure 3: Evolution of the 1D solution for $c = 0.6$.

The evolution of the cross-sections of the 2D solution is the same, because the 2D solution keeps its constant behaviour in the $y-$direction. This constant behaviour of the 2D solution is kept till $y \in [-2.2, 2.2]$, i.e., when $y_{\max} := y_{N_y} \leq 2.2$. When $y_{\max} \geq 2.3$ the 2D solution blows up at finite time.

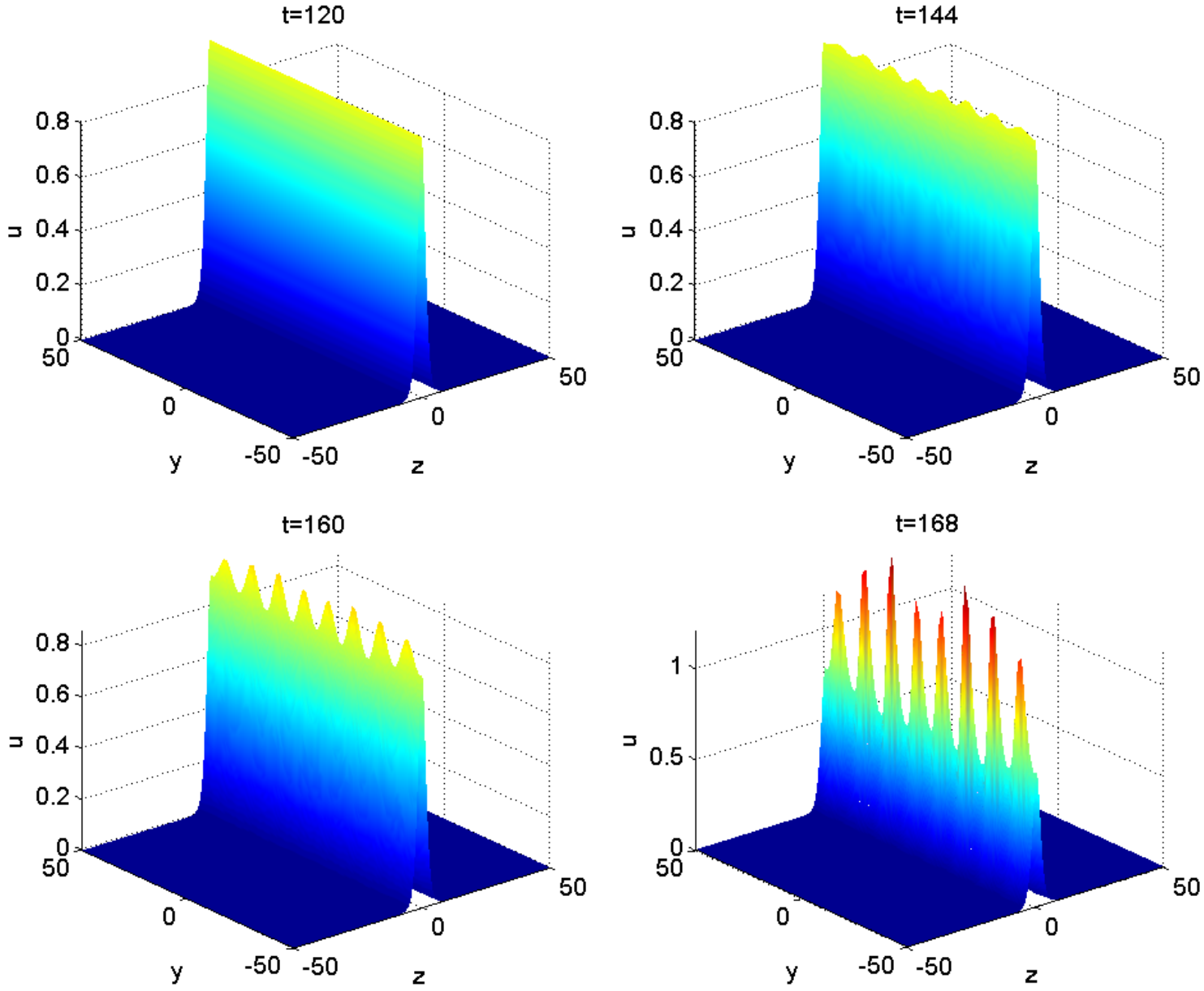

Figure 4: Evolution of 2D solution, $c = 0.6$, $y \in [-50, 50]$, $N_z = 256$, $N_y = 64$.

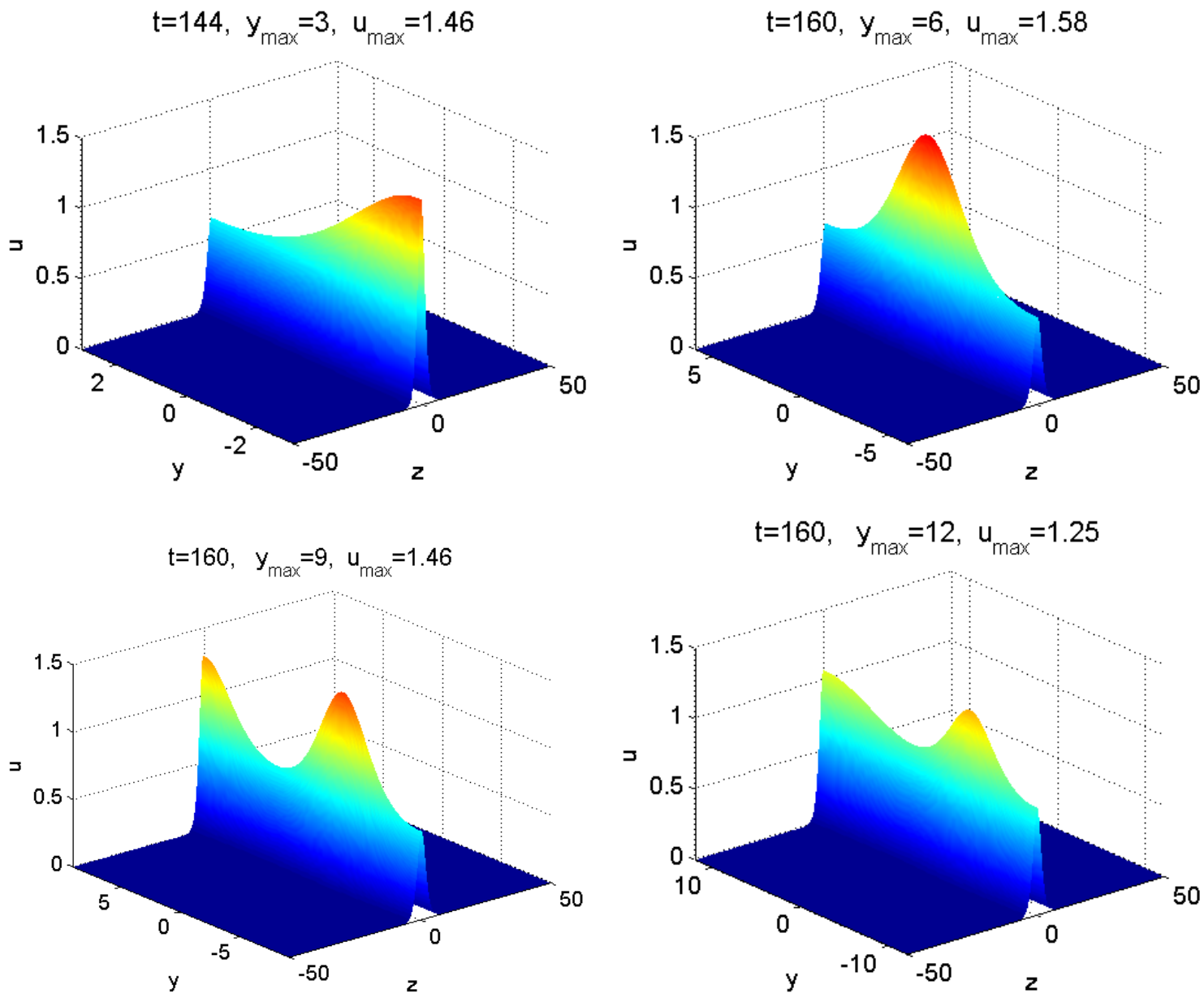

Figure 5: Evolution of 2D solution, $c = 0.6$, different $y_{\max}, N_z = 256, N_y = 64$.

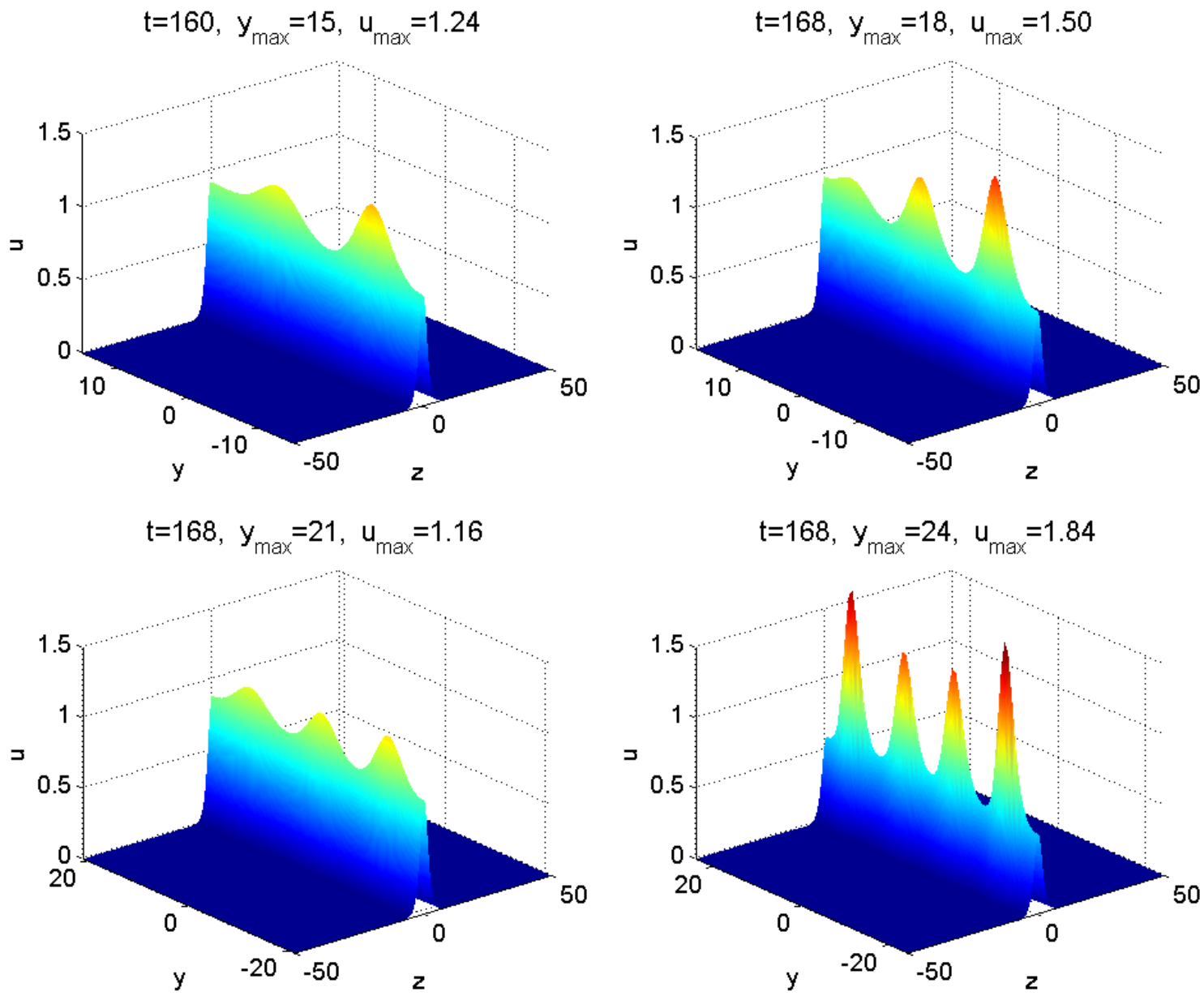

Figure 6: Evolution of 2D solution, $c = 0.6$, different $y_{\max}, N_z = 256, N_y = 64$.

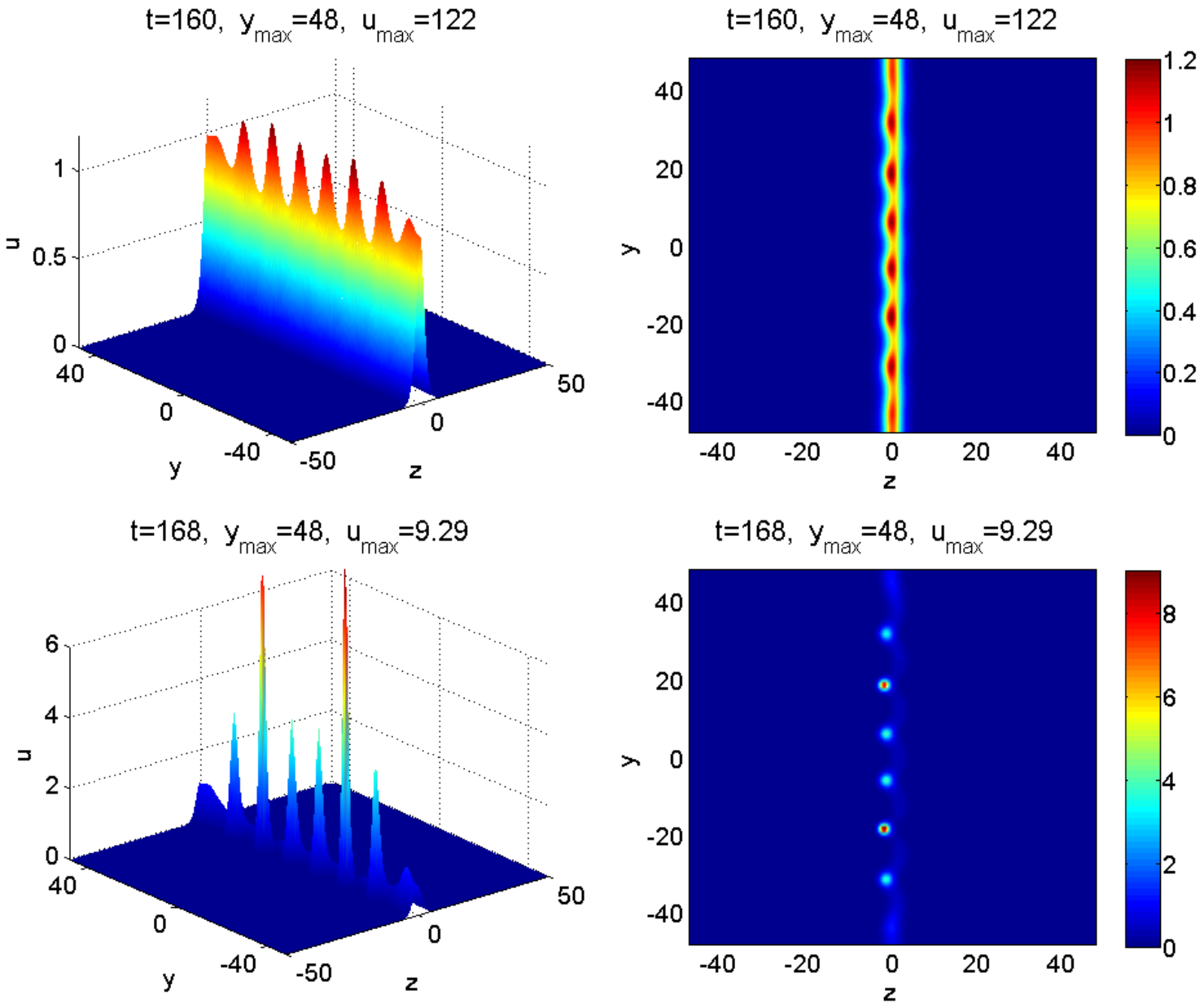

Figure 7: Evolution of 2D solution for $c = 0.6$, $y \in [-48, 48]$, $N_z = 256$, $N_y = 128$.

It seems that the number of the maxima strongly depends on the size of the domain in the y-direction, and radially-symmetric blow-up structures are atractors for some solutions of 2D BPE.

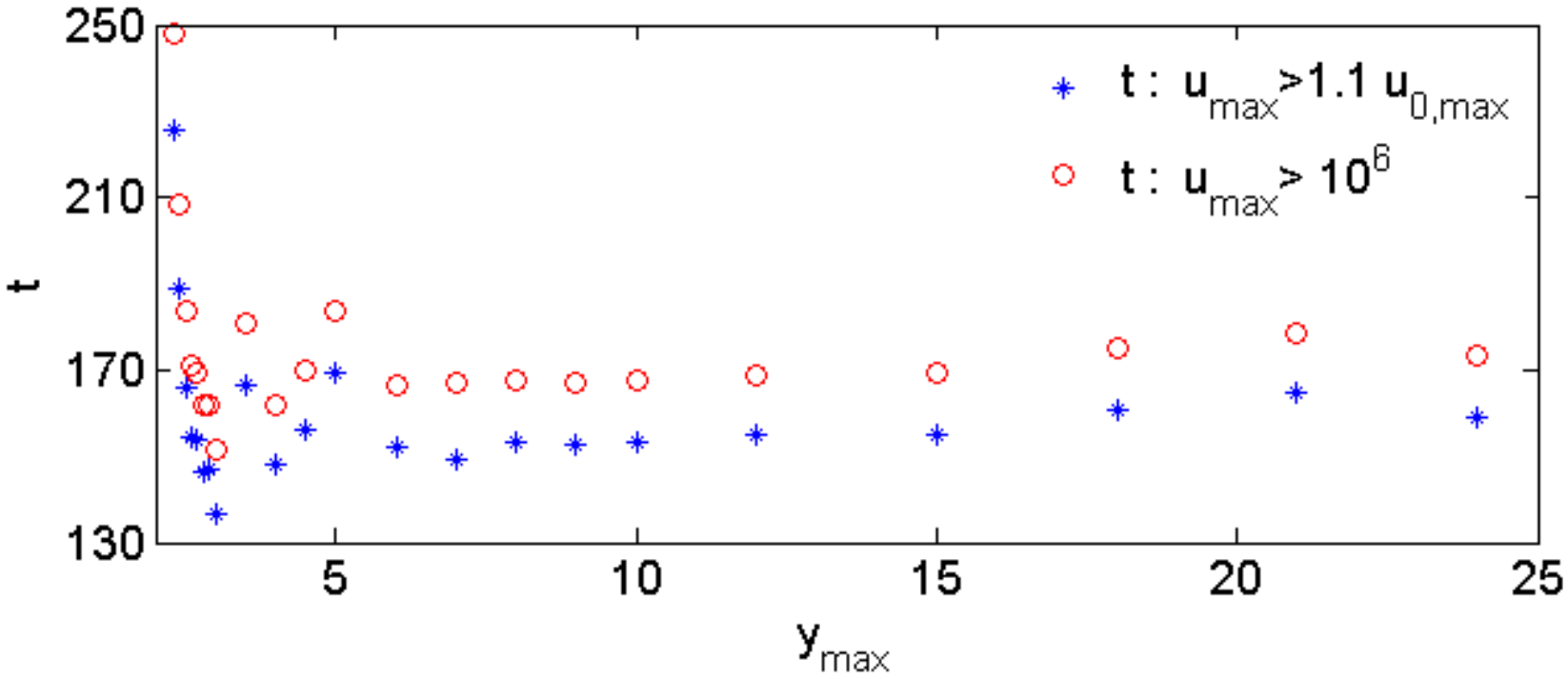

Figure 8: The time of change and the blow-up time for different intervals in y.

Example 3. $c = 0.9$ (1D soliton solution should be stable).

First, results for $(x, y) \in [-50, 50] \times [-1, 1]$ are presented. The behaviour of the solution is quite similar to that for $c = 0.6$ – second order convergence of the solution is demonstrated, there is not any practical difference between both discretisations of the mixed derivative W_{tz}, both approximations of the nonlinear term, and the solution does not depend on the prescribed tolerance for the solution of the linear systems, arising after the discretisation. The difference between the exact and the approximate solution $\delta(U)$ is one and the same for 1D and 2D settings of the problem. The solutions also preserve their shape for very large times $(t = 10^6)$

Table 4: The difference $\delta(U) := \max|U - U^{\text{sech}}|$ between the exact and the numerical solution for $c = 0.9$

	central differences		upwind differences	
t	2D solution	1D solution	2D solution	1D solution
10^2	2.09e-4	2.09e-4	2.09e-4	2.09e-4
10^3	1.64e-3	1.64e-3	1.63e-3	1.63e-3
10^4	3.27e-3	3.27e-3	3.29e-3	3.29e-3
10^5	3.42e-3	3.42e-3	3.33e-3	3.33e-3
10^6	1.81e-3	1.81e-3	2.86e-3	2.86e-3

Table 5: The difference $\delta(U)$ between the exact and the numerical solution, and the order of convergence l for $c = 0.9$

		$t = 400$		$t = 800$		$t = 1200$	
τ	$N_x \times N_y$	$\delta(U)$	l	$\delta(U)$	l	$\delta(U)$	l
0.4	128×8	2.86e-3		5.37e-3		7.05e-3	
0.2	256×16	7.40e-4	1.95	1.33e-3	2.01	2.05e-3	1.78
0.1	512×32	1.88e-4	1.98	3.37e-4	1.99	5.33e-4	1.94

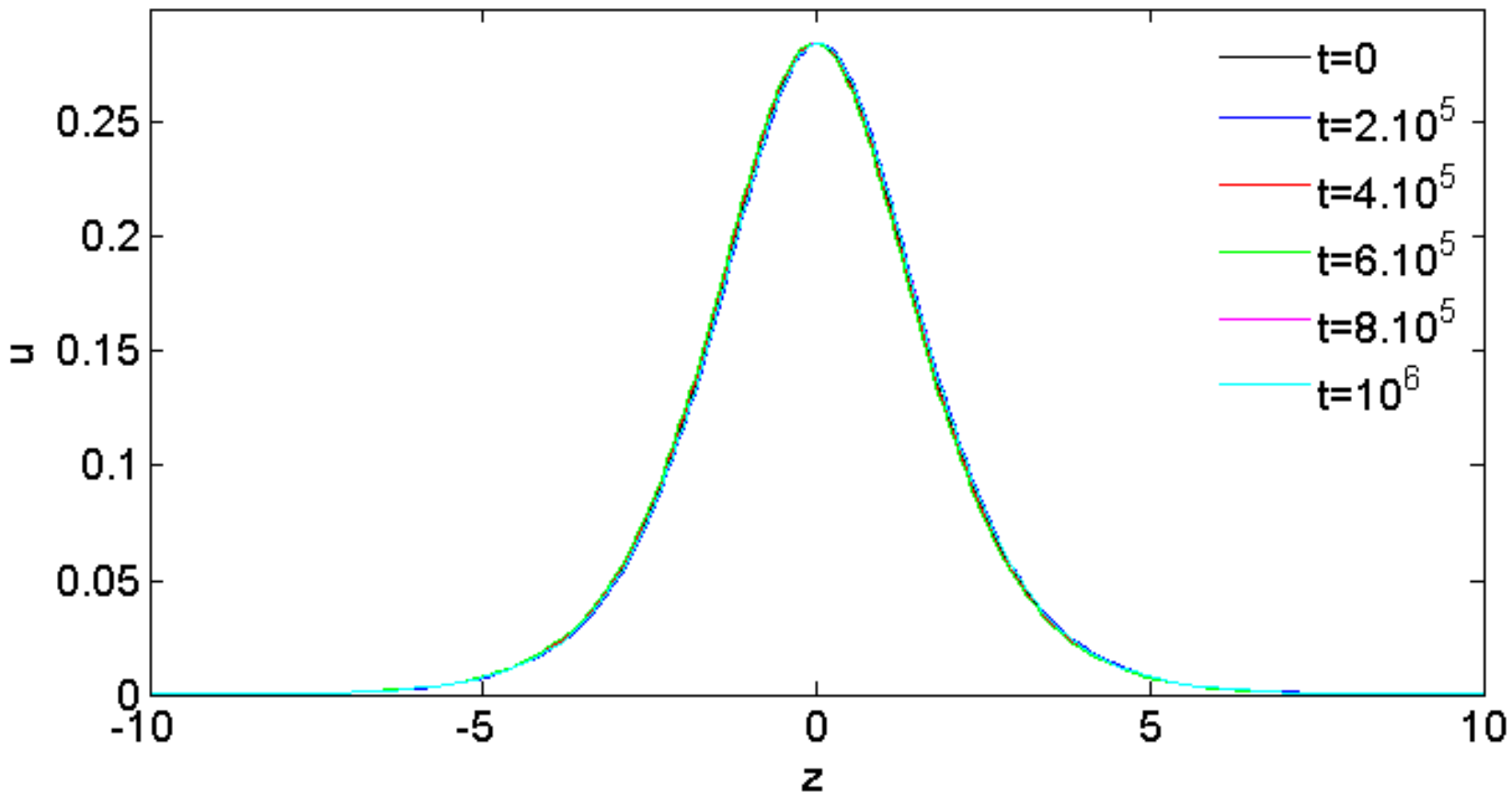

Figure 9: Evolution of the 1D solution for $c = 0.9$.

The evolution of the cross-sections of the 2D solution is the same, because the 2D solution keeps its constant behaviour in the $y-$direction.

This constant behaviour of the 2D solution is kept till $y_{\max} = 7$ on relatively fine grids in the $z-$direction ($N_z = 1024, N_y = 16$) and for $t \leq 10^6$. On relatively coarse grids ($N_z = 256$ or 512) and for relatively large times ($t \approx 5*10^4$ or $2.5*10^5$ for $y_{\max} = 7$) some additional small waves appear in front and behind the main wave. When $y_{\max} \geq 8$ the solution loses its constant behaviour in the $y-$direction. After that some additional small waves may appear near the main wave. These small waves move with a different speed, hit the computational boundary and perturb the solution, i.e., the prescribed boundary conditions for large z are not relevant in such cases.

In order to show second order convergence for larger times, we either need to use very fine grids in the $x-$direction or to impose Dirichlet boundary conditions in the $y-$direction. That is why in the next table we present results with Dirichlet boundary conditions in the $y-$direction and for $y_{\max} = 1$. As can be seen, the errors in this case are much slower and second order convergence is demonstrated up to time $t = 10^6$.

Table 6: The difference $\delta(U)$ between the exact and the numerical solution, and the order of convergence l for $c = 0.9$, in the case of Dirichlet boundary conditions

		$t = 10^2$		$t = 10^4$		$t = 10^6$	
τ	$N_x \times N_y$	$\delta(U)$	l	$\delta(U)$	l	$\delta(U)$	l
central differences							
0.8	64×4	2.56e-4		2.46e-4		2.50e-4	
0.4	128×8	6.31e-5	2.02	6.33e-5	1.96	6.48e-5	1.92
0.2	256×16	1.59e-5	1.99	1.60e-5	1.98	1.55e-5	2.06
upwind differences							
0.8	64×4	2.52e-4		2.42e-4		2.49e-4	
0.4	128×8	6.35e-5	1.99	6.23e-5	1.97	6.31e-5	1.98
0.2	256×16	1.59e-5	2.00	1.58e-5	1.98	1.57e-5	2.01

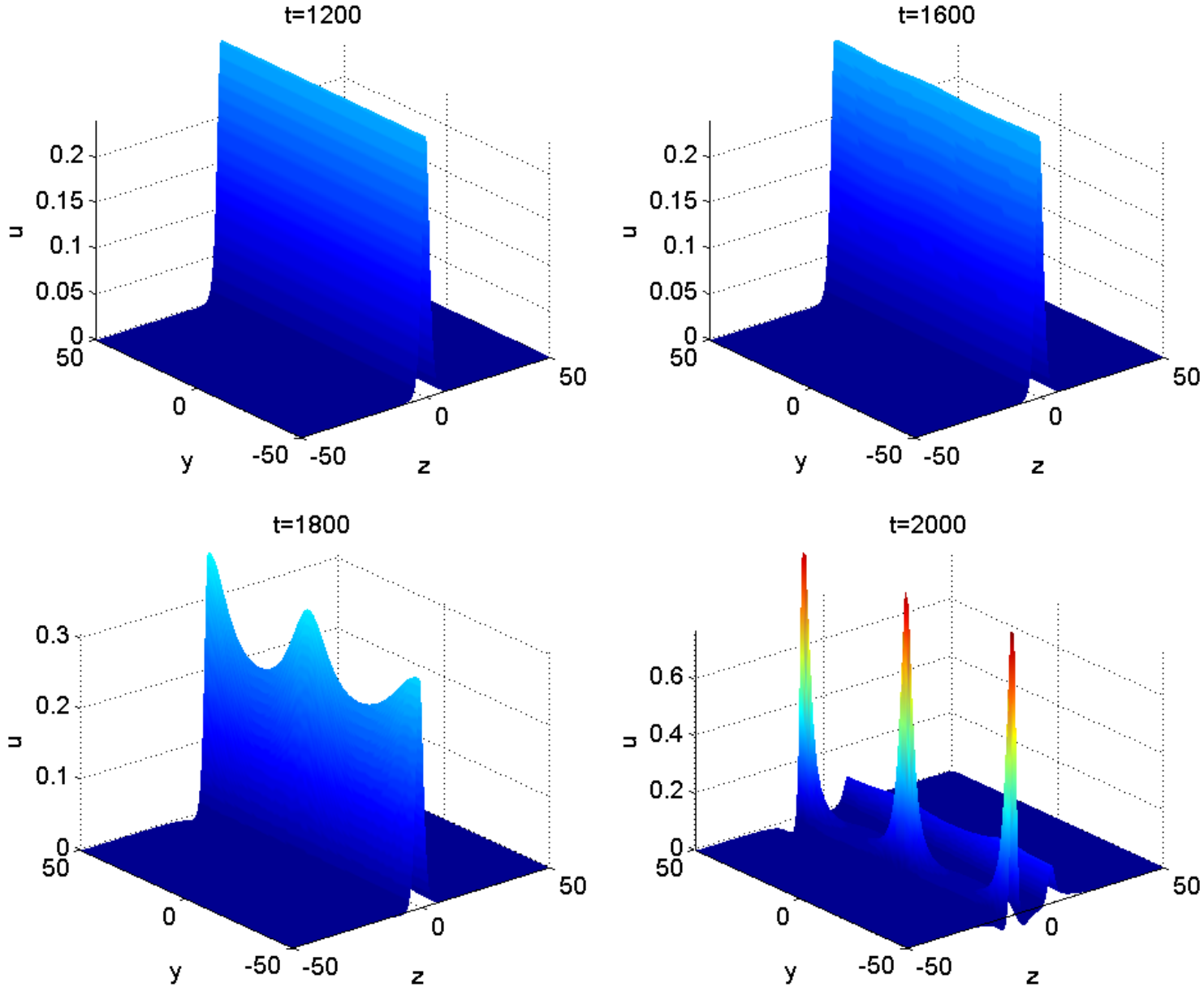

Figure 10: Evolution of 2D solution, $c = 0.9$, $y \in [-50, 50]$, $N_z = 256$, $N_y = 64$.

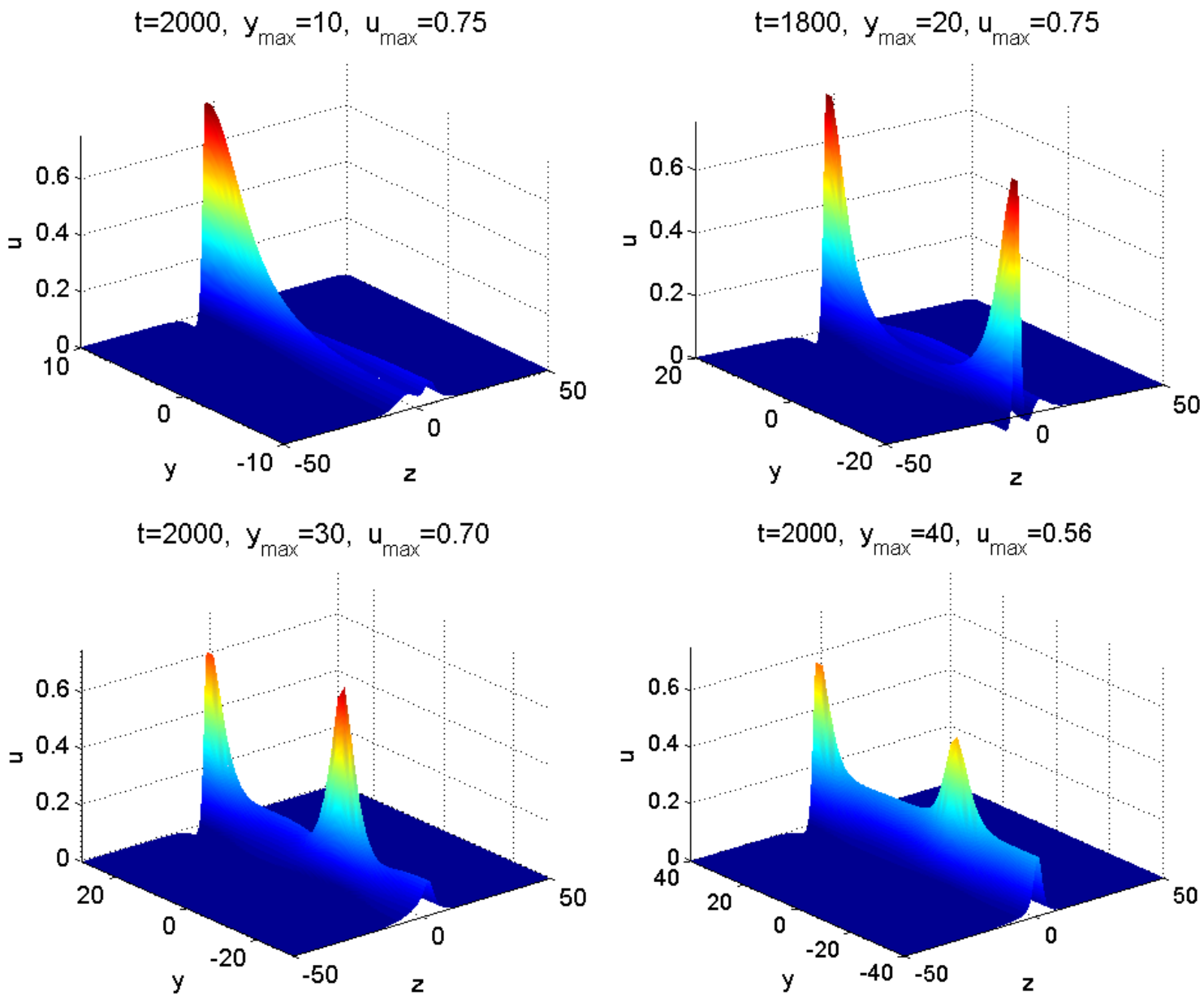

Figure 11: Evolution of 2D solution, $c = 0.9$, different $y_{\max}, N_z = 1024, N_y = 32$.

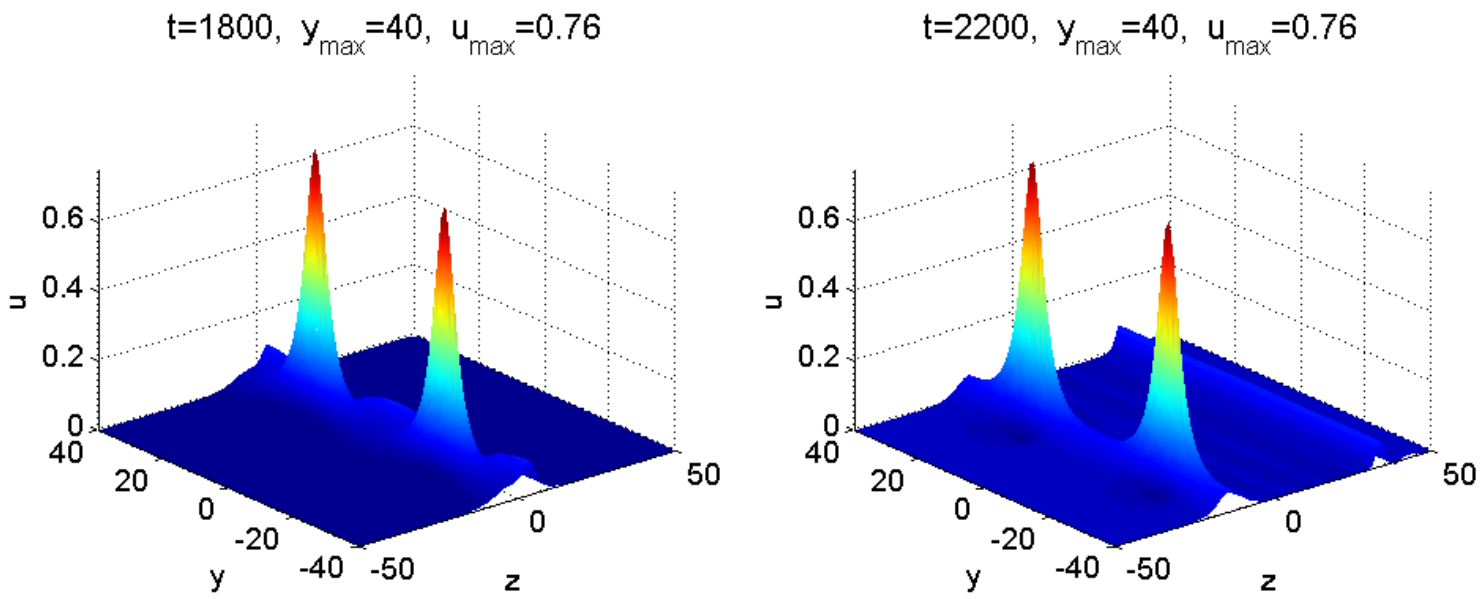

Figure 12: Evolution of 2D solution, $c = 0.9$, different $y_{\max}, N_z = 1024, N_y = 64$.

When the computational region varies in the y-direction, we observe a similar behaviour to that in Example 2. Note, here the number of the maxima for a fixed $y_{\max}$ is essentially smaller then in the previous example. The positions of the maxima may depend on the computational grid (compare results for $y_{\max} = 40$ on the last two figures).

Conclusions

The moving frame coordinate system helps us to keep the localized structure in the center of the coordinate system, where the grid is much finer. It also reduces the effects of the reflection from the boundaries, allows us to use a small computational box and to compute the solution for very large times.

The presented numerical experiments demonstrate the second order of convergence of the schemes. Both discretisations of the mixed derivative W_{tz}, as well as both approximations of the nonlinear term lead to practically one and the same results.

The stable 1D solutions preserve themselves for very large times. The solutions of the 2D problem for the same parameters and in small intervals for y also preserve their shape for very large times.

But the solutions of the 2D problem in large intervals for y seem to be not stable – the waves preserve their shape in relatively long intervals of time (depending on the parameters), but after that the initial shape of the waves is changed. Some smooth oscilations appear in the $y-$direction, and the solutions start to grow. Most probably this effect is due to the instability of the exact solution of the 2D differential problem, even when the corresponding 1D solution is stable.

Let us notice that the implicit time-stepping, used here, introduces some perturbations in the y-direction. Perhaps an explicit method will behave better in this case, but the important open question is about the stability of 2D solitons, i.e., perturbations in the y-directions should be allowed.

Acknowledgment. This work has been supported by Grant DDVU02/71 from the Bulgarian National Science Fund.

Some papers and presentations about BPE may be found at

http://www.math.bas.bg/~nummeth/boussinesq/

Thank you for your attention!